

Lifetime effects on the dissociation of core-excited N<sub>2</sub> and CO molecules

N. Saito,\* A. Hempelmann, F. Heiser,<sup>†</sup> O. Hemmers,<sup>‡</sup> K. Wieliczek, J. Viehhaus, and U. Becker  
*Fritz-Haber-Institut der Max-Planck-Gesellschaft, D-14195 Berlin, Germany*  
 (Received 7 July 1999; published 10 January 2000)

Vibrational-resolved ion and ion-pair yield spectra of N<sub>2</sub> and CO taken at their  $1s \rightarrow \pi^*$  resonance excitations reveal decay-channel-dependent core hole lifetimes. The linewidths of the yield spectra tend to be shortened when the number of electrons ejected in the deexcitation process increases, finally becoming narrower than the total ion yield or absorption natural lifetime width of the core-excited states of N<sub>2</sub> and CO, respectively. In contrast to this, the linewidths of the yield spectra for the singly charged molecular ions, N<sub>2</sub><sup>+</sup> and CO<sup>+</sup>, are shown to be broader than their corresponding natural linewidths. This linewidth shortening and broadening observed in the ion yield spectra are explained by the effect of different internuclear distances on the lifetime of an excited molecular state.

PACS number(s): 33.80.Gj, 33.80.Eh, 33.80.Rv

A core-excited molecule is expected to dissociate in most cases after the molecule is ionized through resonant Auger decay. However, this model was found to be too simple regarding the large variety of potential curves that may be excited. When a core-excited state forms a repulsive potential energy surface, Auger decay competes with the departing motion of atoms in the molecule. Morin and Nenner measured the Auger electron spectrum at the Br 3*d* excitation of HBr [1]. The Auger spectrum includes the very narrow bands, which are attributed to the Auger transitions from the Br atom. This result shows that the core-excited HBr molecule dissociates sometimes faster than the Auger decay. Recently, Menzel *et al.* measured the resonant Auger spectra of HCl, DCl, and Cl<sub>2</sub> following the Cl( $2p_{3/2}$ ) $\rightarrow$ Cl( $\sigma^*$ ) excitation [2], which also has a repulsive potential energy surface. The branching ratio of ‘‘molecular’’ versus ‘‘atomic’’ Auger transitions increases with increasing reduced mass of the target molecules. When the reduced mass of the molecule increases, the departing motion of the atoms in the molecule becomes slower and Auger transitions preferentially occur before complete dissociation. These studies suggest that the dissociation competes with an Auger transition for a core hole excited state with a repulsive potential energy surface. A quantum-mechanical description of this competition was recently given in [3].

In the case of the core-excited states of CO\*( $C1s^{-1}2p\pi$ ) and N<sub>2</sub><sup>\*</sup>( $C1s^{-1}2p\pi_g$ ), ‘‘atomic’’ Auger transitions have not been observed. Since the core-excited states of these molecules form attractive potential energy curves, it is considered that the molecules dissociate after the Auger transitions. However, the molecules have a vibrational motion and the atoms in the molecule move before Auger decay, because the vibration period of N<sub>2</sub><sup>\*</sup>( $1s^{-1}2p\pi_g$ ) amounting to 2.8 fs, is

shorter than the natural lifetime of 5.4 fs of the core-excited state [4]. This atomic motion should be taken into account for the deexcitation of the core-excited molecule, which has an attractive potential energy curve. When a molecule is excited by a photon whose energy is detuned from the resonance energy, the lifetime of the core hole is shortened from the natural lifetime [5]. If deexcitation channels or, in other words, resonant Auger spectra from a core-excited molecule are measured with high-photon-energy resolution, the different lifetime would change the branching ratio of the decay channels. However, since there are many multielectron emission processes from the core-excited molecules, it is impossible to know all these processes from the Auger spectra. Therefore, in the present study, we have measured the final products, i.e., the ion and ion-pair yield spectra from N<sub>2</sub> and CO at their  $1s \rightarrow \pi^*$  resonance excitation with narrow band-path photons. Mass resolved ion yield spectra of core-excited N<sub>2</sub> with vibrational resolution were recently measured using a quadrupole mass spectrometer. However, ion-ion coincidence spectra could not be measured with this method and the same vibrational peaks are not well separated in the spectra. Therefore it is difficult to discuss the effect of the core lifetime on the decay channels from this experiment.

Our experiments were performed at beamline BW3 of the Hamburger Synchrotronstrahlungslabor (HASYLAB) of DESY [7]. This beamline is a triple *N*-pole undulator beamline (*N*=21, 33, 44) equipped with a high resolution SX700 plane grating monochromator modified for high photon throughput. This instrument achieved a bandwidth of about 60 and 70 meV at the photon energies of 300 eV and 400 eV, respectively. Time-of-flight (TOF) mass spectra and ion-ion-coincidence spectra have been measured with a TOF mass spectrometer, comprising a McLaren-type space charge focusing instrument of 42 mm length and a multihit anode [8]. An extraction field of 100 V/mm was applied on the TOF mass spectrometer, which makes it possible to measure all ions and all pairs of charged particles in coincidence, independent of their charge state and initial kinetic energy. The spectrometer was positioned at an angle of 55° with respect to the electric field vector of the photon beam in order to remove the effect of anisotropic fragmentation. The partial

\*Permanent address: Electrotechnical Laboratory, Umezono, Tsukuba-shi, Ibaraki 305-8568 Japan.

<sup>†</sup>Present address: Ericsson Eurolab Deutschland GmbH, Nordostpark 12, 90411 Nürnberg, Germany.

<sup>‡</sup>Present address: Department of Chemistry, University of Nevada, Las Vegas, NV 89154-4003.

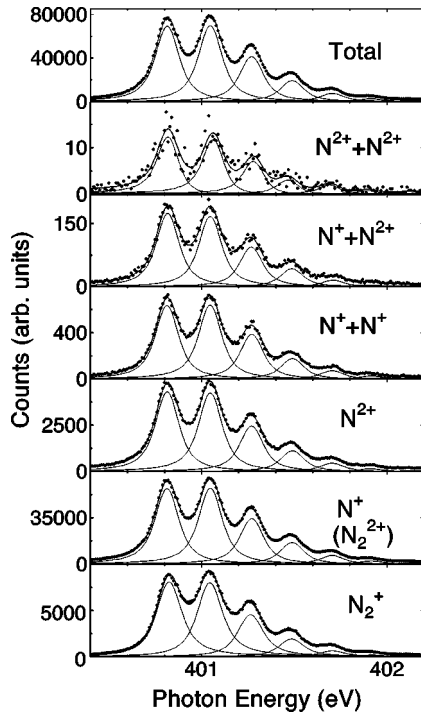


FIG. 1. Ion yield spectra of the total ions,  $N_2^+$ ,  $N^+$ ,  $N^{2+}$ ,  $N^+ + N^+$ ,  $N^+ + N^{2+}$ , and  $N^{2+} + N^{2+}$  taken in the photon energy region of  $N_2(1s) \rightarrow N_2(2p\pi_g)$  photoexcitations. The dots indicate the experimental data and the solid curves are a superposition of Voigt functions reproducing the experimental data.

$N_2$  or CO pressure was lower than  $3 \times 10^{-6}$  mbar. The TOF of the ions was measured with respect to the bunch marker of the storage ring, which was operated in the double-bunch modes with a time window of 482 nsec. The details of this TOF mass spectrometer were described elsewhere [8,9]. In order to avoid possible distortions of the scans, all coincident and noncoincident ionization channels were measured simultaneously during one photon energy scan, including the monitoring of the background in the spectra.

Figure 1 shows the yield spectra of the total ions,  $N_2^+$ ,  $N^+$ ,  $N^{2+}$ ,  $N^+ + N^+$ ,  $N^+ + N^{2+}$ , and  $N^{2+} + N^{2+}$  in the photoexcitation of  $N_2(1s) \rightarrow N_2(2p\pi_g)$ . Several vibrational peaks are seen in the spectra. Solid curves reproduce the experimental data by a fitting calculation using Voigt functions. The conditions of the fitting procedure are as follows: (a) all vibrational peaks in a spectrum have the same Lorentzian linewidth, (b) the Gaussian broadening is the same for all spectra. The Gaussian broadening was 71.0 meV, which was obtained from the fitting calculation for the total ion yield spectrum. The Lorentzian linewidth for the total ion yield spectrum is  $121 \pm 8$  meV, which is close to the natural lifetime broadening reported previously [10–13].

The linewidths of the yield spectra in Fig. 1 are different with respect to each other. The narrow linewidth reflects the large ratio of the peak intensity at  $\nu=0$  to the minimum intensity between  $\nu=0$  and 1. It is clear to state that the linewidth for  $N_2^+$  is the widest and that for  $N^{2+} + N^{2+}$  is the narrowest. Figure 2 shows the Lorentzian linewidths for the ions and the ion pairs. The Lorentzian linewidth becomes

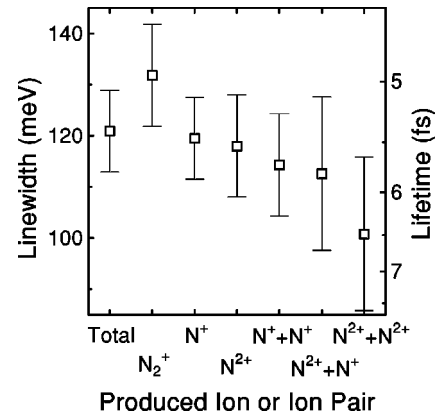


FIG. 2. The Lorentzian linewidths and corresponding lifetimes of the ion or ion-pair yield spectra of  $N_2(1s) \rightarrow N_2(2p\pi_g)$  states.

narrower when the charge state of the ion or ion pair is increased. The Lorentzian linewidth of  $N_2^+$  is broader than the natural lifetime broadening measured by total yield or absorption spectroscopy.

The dependence of the linewidths on the final charge state is also observed in the yield spectra of core excited CO. Figure 3 shows the yield spectra of the total ions,  $CO^+$ ,  $CO^{2+}$ ,  $C^+$ ,  $O^{2+}$ ,  $C^+ + O^+$ , and  $C^{2+} + O^{2+}$  from the  $C1s^{-1}2p\pi$  state of CO. The yield spectra of  $O^+$ ,  $C^{2+}$ ,  $C^+ + O^{2+}$ , and  $C^{2+} + O^+$  are not shown in Fig. 3. The solid curves reproducing the experimental data were derived using

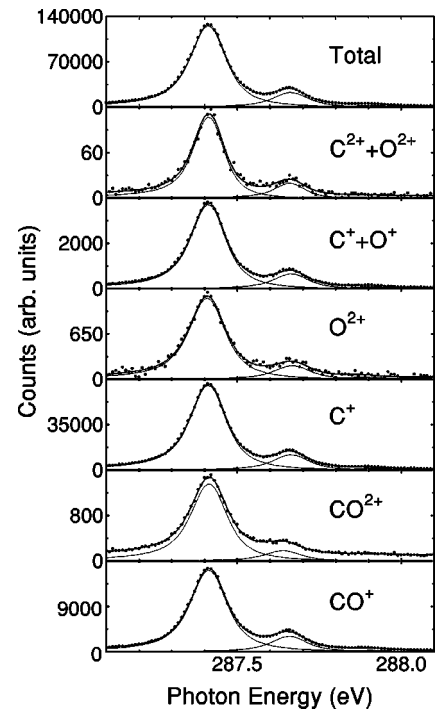


FIG. 3. Ion yield spectra of the total ions,  $CO^+$ ,  $CO^{2+}$ ,  $C^+$ ,  $O^{2+}$ ,  $C^+ + O^{2+}$ , and  $C^{1+} + O^{2+}$  taken in the photon energy region of  $CO(C1s) \rightarrow CO(C2p\pi)$  photoexcitations. The dots indicate the experimental data and the solid curves are a superposition of Voigt functions reproducing the experimental data.

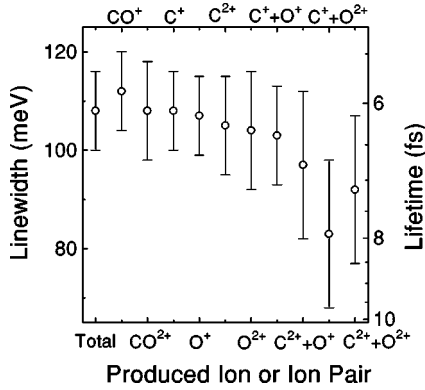


FIG. 4. The Lorentzian linewidths and corresponding lifetimes of the ion or ion-pair yield spectra of  $\text{CO}(C1s) \rightarrow \text{CO}(C2p\pi)$ .

the fitting calculation described above. The Gaussian broadening was deduced to be 58.3 meV by the fitting calculation of the total ion yield spectra. Figure 4 shows the Lorentzian linewidths for the ions and the ion pairs obtained from the fitting calculation. The Lorentzian linewidth for the total ion yield spectrum is  $108 \pm 8$  meV, which is close to the natural lifetime broadening reported previously [12,14,15]. The linewidth generally reduces with increasing charge state of the ion or ion pair.

The present result shows that the characteristic of the Lorentzian linewidths for CO is similar to that for  $\text{N}_2$ . The Lorentzian linewidth becomes narrow with increasing charge state of the final products. In other words, the short lifetime is related to the production of an ion with a lower charge state.

In the following we propose a possible explanation of our result. As described above, the core-excited molecule with an attractive potential energy surface has a vibrational motion within the core lifetime, the atoms in the molecule move, and the internuclear distance of the molecule changes before an Auger transition. This vibrational motion leads to the situation that the transition amplitude of the final products is proportional to the overlapping factor of the excited state and the Auger final-state wave functions. On the other hand, when the core lifetime is shorter than the vibrational period by detuning the photon energy off the resonance, the Auger transitions occur before the atoms in the molecule move. This fixed internuclear distance makes it possible to consider the transition amplitude as proportional to the Franck-Condon factor between ground and Auger final-state wave functions. The transition amplitude is expected to depend on the lifetime or the internuclear distance, which change the branching ratios of the final products correspondingly. Since the latter depend on the core lifetime, the linewidths of the yield spectra depend on the final products.

In order to examine this explanation, the final states of the Auger transitions are discussed below. Core-excited molecules deexcite through electronic transitions and most of them dissociate into fragments. Some of the decay processes that produce ions or ion pairs from the inner-shell excited  $\text{N}_2$  [16–18] and CO [19] are discussed in the papers reported previously. From these studies, the deexcitation schemes of Table I are the dominant ones for a core excited  $\text{N}_2$  molecule.

Pathway (1) of Table I shows that the core-excited  $\text{N}_2$  decays electronically into a molecular ion with an attractive potential energy surface  $\text{N}_2^{n+}$  (AP). It sometimes autoionizes but it does not dissociate, yielding  $\text{N}_2^{n1+}$ . This type of deexcitation process produces  $\text{N}_2^+$  and  $\text{N}_2^{2+}$ . The dissociation scheme (2) of Table I shows that the core-excited  $\text{N}_2$  decays into  $\text{N}_2^{n+}$  (AP) and it sometimes autoionizes and it predissociates into fragments,  $\text{N}^{n1+} + \text{N}^{n2+}$ . Here mainly  $\text{N}^+ + \text{N}$  is produced and  $\text{N}^+ + \text{N}^+$  and  $\text{N}^{2+} + \text{N}$  are only partly generated. Pathway (3) indicates that the core-excited  $\text{N}_2$  decays electronically into the molecular ion  $\text{N}_2^{n+}$  (RP) with a repulsive potential energy surface. It dissociates into the fragments  $\text{N}^{n1+} + \text{N}^{n2+}$ , with or without ejecting an electron. Fragmentation into  $\text{N}^+ + \text{N}^{2+}$  is mainly produced through process (3) and  $\text{N}^+ + \text{N}^+$  and  $\text{N}^{2+} + \text{N}$  are partly produced from this process.

As far as we know, fragmentation into  $\text{N}^{2+} + \text{N}^{2+}$  has not been reported previously. It is mainly considered to take place in process (3). A triply charged molecular ion is produced by an Auger process, and this ion dissociates into  $\text{N}^{2+} + \text{N}^{2+}$  ejecting an electron (like a cascade Auger process). It is possible that a quadruply charged ion produced directly by an Auger process dissociates into  $\text{N}^{2+} + \text{N}^{2+}$ . However, the probability of a four-electron ejection in an Auger process is considered to be much smaller than that of a three-electron ejection; the latter process would be negligible.

In the above discussion of the decay processes, there are three patterns of deexcitation processes: (1) decay into a stable state with an attractive potential energy surface, (2) decay into a state with an attractive potential energy surface and predissociation, (3) decay into a state with a repulsive potential energy surface and dissociation.

Figure 5 shows the schematic potential energy curves of typical Auger final states, the ground state and the excited state of  $\text{N}_2$  together with the Franck-Condon region. The molecule in the ground state ( $X^1\Sigma_g^+$ ) absorbs a photon and it excites into the core-excited state of  $\text{N}_2(1s^{-1}2p\pi_g)$ . Three decay channels from the core-excited  $\text{N}_2$  are indicated in the figure. The first channel is the core-excited  $\text{N}_2$  decaying into the singly charged molecular ion  $\text{N}_2^+(X^2\Sigma_g^+)$ . This molecular ion is stable and does not dissociate. This channel corresponds to the deexcitation scheme (1). The second channel is

TABLE I. Processes (1)–(3) show deexcitation schemes of core-excited nitrogen.

(1)	$\text{N}_2(1s^{-1}\pi^*) \rightarrow \text{N}_2^{n+}(\text{AP}) + ne \rightarrow \text{N}_2^{n1+}$	(+me)	( $n = n1 - m, m = 0, 1$ )
(2)	$\text{N}_2(1s^{-1}\pi^*) \rightarrow \text{N}_2^{n+}(\text{AP}) + ne \rightarrow \text{N}^{n1+} + \text{N}^{n2+}$	(+me)	( $n = n1 + n2 - m, m = 0, 1$ )
(3)	$\text{N}_2(1s^{-1}\pi^*) \rightarrow \text{N}_2^{n+}(\text{RP}) + ne \rightarrow \text{N}^{n1+} + \text{N}^{n2+}$	(+me)	( $n = n1 + n2 - m, m = 0, 1$ )

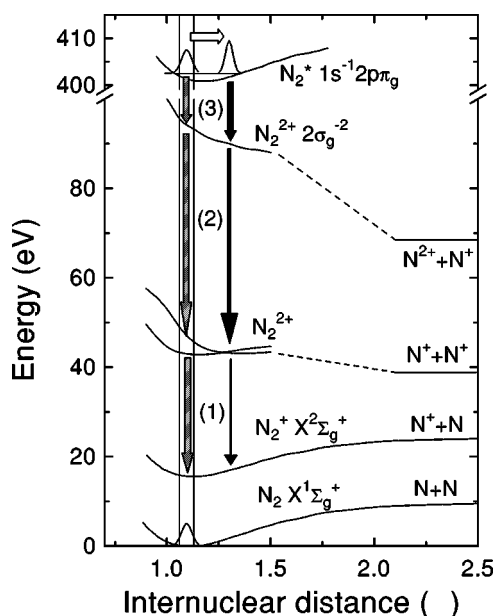


FIG. 5. The schematic diagram of the potential energy curves of the ground state, the core-excited state, and Auger final states of  $N_2$  together with the Franck-Condon region. The hatched arrows indicate the decay channels for a short lifetime of the core hole when the decay takes place in the Franck-Condon region. The solid arrows show the decay channels for a longer lifetime of the core hole decaying outside the Franck-Condon region.

the core-excited  $N_2$  deexciting into a lower level of  $N_2^{2+}$ , which remains a molecular ion or dissociates into  $N^+ + N^+$  [16,20]. The processes of (1), (2), and (3) are mixed in this pathway. The third channel is  $N_2(1s^{-1}2p\pi_g)$  deexciting to the excited doubly charged molecular ion  $N_2^{2+}(2\sigma_g^{-2})$ . This doubly charged ion is not stable and dissociates into  $N^{2+} + N^+$  with ejecting an electron [16]. This deexcitation corresponds to process (3).

The internuclear equilibrium distances of  $N_2$  and  $N_2^+$  are 1.0977 Å and 1.1164 Å, respectively, which are shorter than that of the core-excited  $N_2^*$  amounting to 1.164 Å [10–13,21]. When the core hole is filled faster than the vibrational motion takes place, the Auger transitions occur in the Franck-Condon region (transitions of the hatched arrows). If the lifetime of the core hole is longer than the vibrational motion, deexcitation processes also occur out of the Franck-Condon region (transitions of the solid arrows).

Let us now consider the effect of the core hole lifetime on the transition amplitude of  $N_2 \rightarrow N_2^* \rightarrow N_2^+$ , which corresponds to process (1). The transition amplitude is proportional to the Franck-Condon factor between the ground and Auger final-state wave functions for the short lifetime of the core hole. On the other hand, the transition amplitude is proportional to the overlapping factor between the excited and Auger final-state wave functions for the long lifetime. In this process, the equilibrium distance of  $N_2$  is close to that of  $N_2^+$  but not close to that of  $N_2^*$ . Therefore, the Franck-Condon factor between  $N_2$  and  $N_2^+$  is considered to be larger than the overlapping factor of  $N_2^*$  and  $N_2^+$ . This in-

dicates that the transition amplitude into  $N_2^+$  decreases with an increasing lifetime of the core hole. The effect of the lifetime on the transition amplitude for process (2) is similar to process (1), because after an Auger transition the molecule has an attractive potential and the internuclear equilibrium distance of the Auger final state is close to that of the ground state.

Next, the effect of the core hole lifetime on the transition amplitude of the process  $N_2 \rightarrow N_2^* \rightarrow N_2^{2+} \rightarrow N^{2+} + N^+$  [process (3)] is considered. Since the potential energy curve of  $N_2^{2+}$  in this process is repulsive, the Franck-Condon factor between the ground and final states is not considered to be much different from the overlapping factor between the excited and final states. The transition amplitude does not depend on the lifetime of the core hole.

From the above consideration, processes (1) and (2) are enhanced for the short lifetime of the core hole, whereas process (3) is enhanced for the long lifetime. When the photon energy is tuned slightly off the resonance, the lifetime of the core hole becomes shorter. Then, the amplitudes of processes (1) and (2) off the resonance become relatively higher than that of process (3). In contrast, the branching ratio of process (3) increases on the resonance because the lifetime of the core hole becomes longer. Due to this the linewidths of yield spectra from processes (1) and (2) are wider than those from process (3).

Since the molecular ion  $N_2^+$  is produced in process (1), the linewidth of this ion yield spectrum becomes wider than that of other ion yield spectra. The  $N^+$  ion is mainly produced by fragmentation into  $N^+ + N$  and  $N^+ + N^+$ . Fragmentation into  $N^+ + N$  mainly occurs in process (2) and  $N^+ + N^+$  results from both processes (2) and (3). Then, the linewidth of the  $N^+$  yield spectra is the second widest. Fragmentation into  $N^{2+} + N^{2+}$  mainly occurs in process (3), yielding the narrowest linewidth of the yield spectrum.

The same explanation is adapted to the linewidth variation of the ion yield spectra from core-excited CO because the internuclear equilibrium distances of CO and  $CO^+$  are 1.1283 Å and 1.115 Å, respectively, i.e., shorter than that of  $CO^*(C1s^{-1}2p\pi)$  with 1.1529 Å [5].

In summary, the linewidths of our measured yield spectra tend to shorten with increasing number of electrons ejected in the deexcitation process. The linewidths of the yield spectra for the singly charged molecular ions  $N_2^+$  and  $CO^+$  are broader than the natural lifetime broadening of the core-excited states of  $N_2$  and CO, respectively. These linewidth variations are explained by the lifetime dependence of the deexcitation processes along with the change of the internuclear distance of the molecule. Since the natural lifetime of the  $N_2$  and CO core holes is longer than the vibrational motion, an Auger decay from the core-excited states occurs not only in the Franck-Condon region but also in the vibrational region of the core-excited state. However, when the photon energy is tuned off the resonance, the lifetime of the core hole becomes shorter than the natural lifetime, which forces the core-excited molecule more likely to decay in the Franck-Condon region. The lifetime difference, which is induced by tuning the photon energy, changes the population



of the deexcitation channels, and, consequently, the line-widths of the yield spectra of the fragmentation products.

This research was funded by the Bundesministerium für Bildung, Wissenschaft, Forschung und Technologie (BMBF)

and the Deutsche Forschungsgemeinschaft. N.S. is grateful to the Alexander von Humboldt Foundation for financial assistance. F.H. acknowledges financial support by the Deutscher Akademischer Austauschdienst.

- 
- [1] P. Morin and I. Nenner, *Phys. Rev. Lett.* **56**, 1913 (1986).
- [2] A. Menzel, B. Langer, J. Viefhaus, S. B. Whitfield, and U. Becker, *Chem. Phys. Lett.* **258**, 265 (1996).
- [3] Z. W. Gortel, R. Teshima, and D. Menzel, *Phys. Rev. A* **60**, 2159 (1999).
- [4] C. T. Chen, *Nucl. Instrum. Methods Phys. Res. A* **256**, 595 (1987); C. T. Chen and F. Sette, *Rev. Sci. Instrum.* **60**, 1616 (1989).
- [5] S. Sundin, F. Kh. Gel'mukhanov, H. Ågren, S. J. Osborne, A. Kikas, O. Björneholm, A. Ausmees, and S. Svensson, *Phys. Rev. Lett.* **79**, 1451 (1997).
- [6] A. Karawajczyk, *Phys. Scr.* **53**, 46 (1996).
- [7] A. R. B. de Castro and R. Reining, *Rev. Sci. Instrum.* **63**, 1317 (1992); C. U. S. Larsson, A. Beutler, O. Björneholm, F. Federmann, U. Hahn, A. Rieck, S. Verbin, and T. Möller, *Nucl. Instrum. Methods Phys. Res. A* **337**, 603 (1994).
- [8] N. Saito, F. Heiser, O. Hemmers, K. Wieliczek, J. Viefhaus, and U. Becker, *Phys. Rev. A* **54**, 2004 (1996).
- [9] N. Saito, F. Heiser, O. Hemmers, A. Hempelmann, K. Wieliczek, J. Viefhaus, and U. Becker, *Phys. Rev. A* **51**, R4313 (1995).
- [10] C. T. Chen, Y. Ma, and F. Sette, *Phys. Rev. A* **40**, 6737 (1989).
- [11] G. C. King, F. H. Read, and M. Tronc, *Chem. Phys. Lett.* **52**, 50 (1977).
- [12] A. P. Hitchcock and C. E. Brion, *J. Electron Spectrosc. Relat. Phenom.* **18**, 1 (1980).
- [13] A. Kivimäki, K. Maier, U. Hergenbahn, M. N. Piancastelli, B. Kempgens, A. Rüdell, and A. M. Bradshaw, *Phys. Rev. Lett.* **81**, 301 (1998).
- [14] M. Tronc, G. C. King, and F. H. Read, *J. Phys. B* **12**, 137 (1979).
- [15] D. A. Shaw, G. C. King, D. Cvejanovic, and F. H. Read, *J. Phys. B* **17**, 2091 (1984).
- [16] N. Saito and I. H. Suzuki, *Chem. Phys. Lett.* **129**, 419 (1986); *J. Phys. B* **20**, L785 (1987); *Int. J. Mass Spectrom. Ion Processes* **82**, 61 (1988).
- [17] I. H. Suzuki and N. Saito, *J. Chem. Phys.* **91**, 5324 (1989).
- [18] W. Eberhardt, E. W. Plummer, I. W.-Lyo, R. Carr, and W. K. Ford, *Phys. Rev. Lett.* **58**, 207 (1987).
- [19] A. P. Hitchcock, P. Lablanquie, P. Morin, E. Lizon, A. Lugin, M. Simon, P. Thiry, and I. Nenner, *Phys. Rev. A* **37**, 2448 (1988).
- [20] R. W. Wetmore and R. K. Boyd, *J. Chem. Phys.* **90**, 5540 (1986).
- [21] A. A. Radzig and B. M. Smirnov, *Reference Data on Atoms, Molecules, and Ions* (Springer-Verlag, Berlin, 1985).